European Journal of Human Genetics (2019) 27:389–399
https://doi.org/10.1038/s41431-018-0294-0

ARTICLE

Assessment of fibroblast nuclear morphology aids interpretation of *LMNA* variants

Florence H. J. van Tienen[1,2] · Patrick J. Lindsey[3] · Miriam A. F. Kamps[2,3] · Ingrid P. Krapels[1] · Frans C. S. Ramaekers[2,3] · Han G. Brunner[1,4] · Arthur van den Wijngaard[1] · Jos L. V. Broers[3,5]

Received: 1 March 2018 / Revised: 12 October 2018 / Accepted: 16 October 2018 / Published online: 12 November 2018
© European Society of Human Genetics 2018

Abstract

The phenotypic heterogeneity of Lamin A/C (*LMNA*) variants renders it difficult to classify them. As a consequence, many *LMNA* variants are classified as variant of unknown significance (VUS). A number of studies reported different types of visible nuclear abnormalities in *LMNA*-variant carriers, such as herniations, honeycomb-like structures and irregular Lamin staining. In this study, we used lamin A/C immunostaining and nuclear DAPI staining to assess the number and type of nuclear abnormalities in primary dermal fibroblast cultures of laminopathy patients and healthy controls. The total number of abnormal nuclei, which includes herniations, honeycomb-structures, and donut-like nuclei, was found to be the most discriminating parameter between laminopathy and control cell cultures. The percentage abnormal nuclei was subsequently scored in fibroblasts of 28 *LMNA* variant carriers, ranging from (likely) benign to (likely) pathogenic variant. Using this method, 27 out of 28 fibroblast cell cultures could be classified as either normal ($n = 14$) or laminopathy ($n = 13$) and no false positive results were obtained. The obtained specificity was 100% (CI 40–100%) and sensitivity 77% (46–95%). We conclude that assessing the percentage of abnormal nuclei is a quick and reliable method, which aids classification or confirms pathogenicity of identified *LMNA* variants causing formation of aberrant lamin A/C protein.

Introduction

LMNA variants can cause a plethora of phenotypes that are collectively called laminopathies [1]. At least 12 different types can be distinguished [1], presenting as multi-organ systemic diseases or as tissue-specific diseases. Systemic diseases are often due to sporadic variants that lead to severe clinical symptoms such as Hutchinson Gilford Progeria Syndrome (HGPS) causing premature ageing [2]. In rare cases, compound heterozygous variants can lead to a recessive Progeria phenotype [3]. Tissue-specific laminopathies are much more common, and include Emery Dreifuss Muscular dystrophy (EDMD), Dunnigan type familial partial lipodystrophy (FPLD2), limb girdle dystrophy, and dilated cardiomyopathy (DCM). Genotype-phenotype correlations have not yet been fully resolved. On the one hand, different tissues can be affected in laminopathies arising from a single point variant, leading to overlapping syndromes [4]. Even within a single family, different phenotypes can be found. As example, patients carrying an identical *LMNA* variant were diagnosed as having DCM, DCM with Emery-Dreifuss muscular dystrophy (EDMD)-like symptoms and DCM with limb girdle muscular dystrophy (LGMD)-like symptoms [5].

The genetic heterogeneity of DCM in combination with phenotypic heterogeneity and variable penetrance of *LMNA* variants complicates *LMNA* variant classification.

These authors contributed equally: Florence H.J. van Tienen, Jos L.V. Broers

✉ Florence H. J. van Tienen
Florence.van.tienen@mumc.nl

1 Department of Clinical Genetics, Maastricht University Medical Centre, Maastricht, The Netherlands

2 GROW-School for Oncology and Developmental Biology, Maastricht University Medical Centre, Maastricht, The Netherlands

3 Department of Genetics and Cell Biology, Maastricht University Medical Centre, Maastricht, The Netherlands

4 Department of Human Genetics, Radboud University Medical Center, Nijmegen, The Netherlands

5 CARIM-School for Cardiovascular Diseases, Maastricht University Medical Centre, Maastricht, The Netherlands

Following the guidelines of the American College of Medical Genetics and Genomics [6], *LMNA* variants are often classified as variant of unknown significance (VUS) in the absence of segregation and/or functional data from the literature. A VUS neither explains, nor excludes a clinical diagnosis, which poses challenges for patient counseling. In order to study the functional effect of *LMNA* variant, a number of groups have assessed the nuclear structure of fibroblasts from *LMNA*-mutated persons and linked nuclear abnormalities in dermal fibroblasts with the type of variant, and disease phenotype [7–13]. While most laminopathy cell cultures showed nuclear abnormalities, such as nuclear herniations (blebs) and/or irregularities in lamin staining, seen as honeycomb structures, it was difficult to correlate these nuclear abnormalities with the type of the variant, location in the protein or disease status [13]. In this paper we describe the development of a simple analysis procedure using lamin A/C immunostaining and DAPI staining to assess nuclear morphology. Combined with linear regression analysis, it can be determined whether a fibroblast culture qualifies as laminopathy and herewith this method will aid to the classification of *LMNA* variants based on nuclear morphology analysis of the patients' dermal fibroblasts.

Materials and methods

Cell culture

Human dermal fibroblast cultures were obtained from dermal biopsies after written informed consent as described previously [14]. Anonymous control fibroblasts were obtained from healthy individuals or individuals with a variant in a gene that is not expressed in fibroblasts, e.g., *SCN5A* or *MYH7*. Whenever possible, fibroblasts were stained at a low passage number (mean 3.4 ± 1.1, range p2–p7). Cells were seeded onto 18 mm round glass coverslips (Menzel) without coating and grown for 48 h to a confluence of 50–75%. Cells were fixed in 100% methanol for 15 min at −20 °C and were stored at 4 °C in PBS containing 0.01% Na-azide until use.

Genetic analysis

Sanger sequencing or next-generation sequence analysis and interpretation of *LMNA* (NG_008692.2; NM_170707.3), *SCN5A* (NG_008934.1; NM_198056.2) and *MYH7* (NG_007884.1; NM_00257.3); *EMD* (NG_08677.1; NM_000117.2) gene variants was performed as described previously [15]. A VUS or (likely) pathogenic variant in *LMNA* was excluded in control fibroblasts. Initial classification of identified *LMNA* variants was performed in line with the ACMG standards and guidelines [6]. All reported variants have been uploaded into the publically available LOVD database (https://databases.lovd.nl/shared/genes/LMNA), patient IDs: 165,050; 165,051; 165,052; 165,045; 165,042; 165,053; 165,054; 165,044; 164,979; 164,980; 164,981; 165,048; 165,003; 165,047; 164,804; 165,023; 164,810; 165,005–165,009; 165,029; 165,031; 165,010; 165,012; 165,011; 165,019; 165,046; 165,016; 181,217–181,221.

Immunofluorescence

All samples were pre-incubated in PBS containing 3% BSA (Roche Diagnostics, Mannheim, Germany) and then incubated for 60 min with primary monoclonal antibody JoL2 for Lamin A/C [16] (IgG1, kindly provided by C. Hutchison, University of Durham, UK) 1:50 diluted in PBS containing 3% BSA. Alternatively, a Lamin A mouse monoclonal antibody 133A2 (IgG3, Nordic-MUbio, Susteren, The Netherlands, diluted 1:1000); or Lamin C specific rabbit polyclonal antibody RalC, (Nordic-MUbio, Susteren, The Netherlands, diluted 1:500) were used.

After washing with PBS, FITC conjugated rabbit anti-mouse Ig antibody (Dakopatts, Glostrup, DK) diluted 1:100 in PBS/BSA was applied and incubated for 60 min. After another series of washing steps in PBS, cells were mounted in 90% glycerol, containing 20 mM Tris–HCl pH 8.0, 0.02% NaN_3, 2% 1,4-di-azobicyclo-(2,2,2)-octane (DABCO; Merck, Darmstadt, Germany), and diamidino-2-phenylindole (DAPI; 0.5 µg/ml Sigma-Aldrich).

Detection of nuclear abnormalities

For every patient's fibroblast culture at least 2 × 100 cells in different areas of the sample were evaluated using a Leica DMRBE fluorescence microscope (Leica, Mannheim, Germany), equipped with a 63x oil objective (Plan Apo, NA 1.32). Different aspect of the nuclear morphology were assessed, i.e., presence of nuclear shape abnormalities, seen as irregular lining of the nuclear membrane, forming nuclear blebs (herniations), extensive lobulations or donut-like invaginations of the nucleus. In addition, Lamin staining abnormalities were scored, including extranuclear staining, and the presence of so-called honeycombs. Also, the intensity of staining was registered as being weak, moderate or strongly positive. Part of the samples were re-counted independently by a second examiner, revealing that only a limited inter-observer variation was found (variation 1.09 ± 0.25% ($n = 7$) (mean ± SEM). Finally, the presence of intranuclear

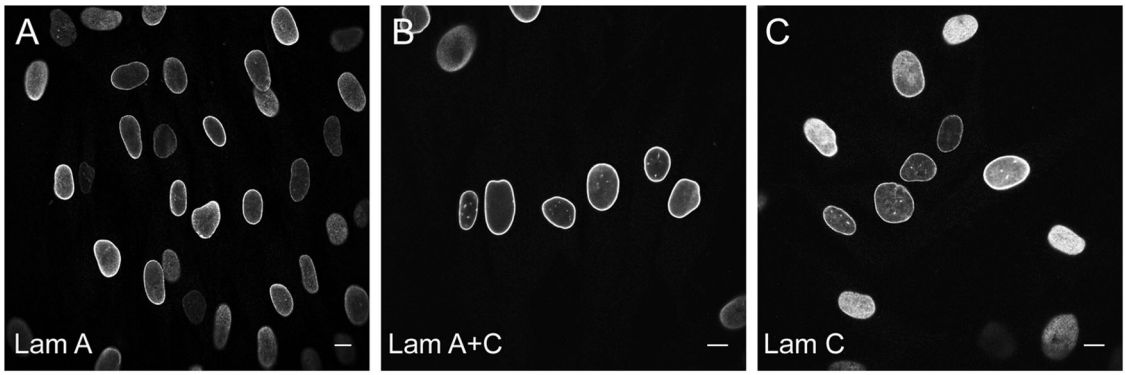

Fig. 1 Immunofluorescence labeling of control fibroblast cells with different A-type lamin antibodies. **a** Lamin A antibody 133A2; **b** lamin A + C antibody JoL2; **c** lamin C antibody RalC

aggregates was registered, after excluding intranuclear invaginations that are common also in normal fibroblasts.

Statistical analyses

A linear logistic regression model was constructed to classify the controls versus the laminopathy patients. A hierarchical model was built allowing for the percentage of normal cells, or cells with blebs, honeycombs, or donut cells present to be taken into account. The inference criterion used for comparing the models is their ability to predict the observed data, i.e., models are compared directly through their minimized minus log-likelihood. When the numbers of parameters in models differ, they are penalized by adding the number of estimated parameters, a form of the Akaike information criterion (AIC) [17]. All statistical analysis presented were performed using the freely available program R [18]. The formula: round(1−(1/(1 + exp (−145.1 + 1554.9 × total abnormal count/total cCount))),2) was generated in order to classify a fibroblast cell-line as "laminopathy" or "normal".

Results

Determination of the "nuclear morphology classifier"

For morphological analysis, different *LMNA* antibodies detecting lamin A only; lamin A and lamin C; and lamin C only, were initially tested. As shown in Fig. 1, similar results were obtained with all three antibodies. Lamin A showed in general a relative homogeneous staining reaction in all nuclei, while the lamin C antibody showed a more heterogeneous labeling. The lamin A + C antibody shows an intermediate staining pattern. While some variations in intensity levels occurred, none of the patient samples examined showed a clear differential expression between lamin A and C. Nuclei, not showing any lamin staining were not detected. Therefore, for further development of the nuclear morphology classifier, only the JoL-2 antibody (recognizing both lamin A and lamin C) and DAPI for nuclear counterstaining were used.

The morphology of ≥200 nuclei per cell culture was analyzed for all 8 controls and 9 fibroblast cultures with a *LMNA* variant that were published previously and designated as pathogenic and laminopathy based on clinical phenotype, segregation data and/or functional analyses (Table 1). In addition to classifying nuclei as normal or abnormal, the types of nuclear malformations were noted: blebs (herniations, including micronuclei), honeycomb structures, donut-like structures, or combinations of aforementioned categories (see Fig. 2; Table 2). In some cultures, intra-nuclear aggregates occurred next to a normal lamina staining (Fig. 3). However, since these aggregates varied dramatically in size as well as in number between cells within the same culture and were even noted in some normal cells, cells with aggregates were not included in the classifier. Statistical analyses of these parameters for the healthy and laminopathy cell-lines were conducted to determine the most discriminating parameter. As shown in Table 3, the parameter "percentage of abnormal nuclei" resulted in the lowest AIC, and was therefore most discriminative and used for subsequent analyses. Using this parameter, the eight control cell-lines showed on average 4.8 ± 1.0% abnormal nuclei (range 3.3–6%) and the nine laminopathy samples showed 26.3 ± 13.6% abnormal nuclei (range 10.6–53%).

Validation study "nuclear morphology classifier"

As noted above, the percentage of abnormal nuclei was identified as the most discriminating parameter between laminopathy and control cells. Subsequently, a validation study comprising nuclear morphology analysis of 28 fibroblast cell-lines was performed and verified by second

Table 1 Overview of published laminopathy fibroblasts used in this study

ID	LMNA nucleotide[a]	Predicted potein change	Zygosity	Phenotype[b]	References[c]
1	c.94_96del	p.(Lys32del)	Heterozygous	EDMD	[13, 29]
2	c.777T > A	p.(Tyr259*)	Homozygous	Died shortly after birth	[30–32]
3	c.992G > A	p.(Arg331Gln)	Heterozygous	DCM	[33–35]
4	c.1315C > T	p.(Arg439Cys)	Heterozygous	FPLD	[20, 31, 36]
5	c.1444C > T	p.(Arg482Trp)	Heterozygous	FPLD	[10, 36, 37]
6	c.1583C > T	p.(Thr528Met)	Heterozygous	DCM	[3, 31, 38]
7	c.[1583C > T]; [1619T > C]	p.[(Thr528Met)]; [(Met540Thr)]	Compound heterozygous	HGPS	[3, 31, 38]
8	c.1609-12T > G	p.(Glu537Val_fs*14)	Heterozygous	Heart-Hand syndrome	[39]
9	c.1824C > T	cryptic splice donor: p.(Gly607_656del)	Heterozygous	HGPS	[40–42]

[a]LMNA NG_008692.2 NM_170707.3

[b]Phenotype abbreviations: *EDMD* Emery Dreifuss muscular dystrophy, *DCM* dilated cardiomyopathy, *FPLD* familial partial lipodystrophy, *HGPS* Hutchinson Gilford Progeria syndrome

[c]References are limited to maximal three per variant; additional publications are available via HGMD website [58]

opinion from expert (Fig. 4). These cell-lines contained a *LMNA* variant that was classified by molecular genetics criteria as (likely) benign, variant of unknown significance (VUS), likely pathogenic variant or pathogenic variant (Table 4). The number of normal and abnormal nuclei per cell culture was determined according to the "nuclear morphology classifier". A cell culture with a classifier score ≥0.95 was considered as "laminopathy" and a value of ≤0.05 was considered as "normal". If the classifier value ranged between 0.05 and 0.95, the cell-line was considered as "unclassified". As shown in Table 4, 27 out of the 28 cell-lines (96%) could be classified with ≥95% probability as laminopathy or normal nuclear morphology. Only ID 37, containing a *LMNA* VUS c.1634G>A ((p.(Arg545His)), had a score of 51% and could therefore not be classified. Out of the 27 classified cell-lines, 13 were defined as laminopathy and 14 as normal. The laminopathy group contained fibroblasts with either a pathogenic variant ($n = 1$), a likely pathogenic variant ($n = 8$) or a VUS ($n = 4$). The group classified as normal mainly contained VUS cell cultures ($n = 8$), two cell cultures with a (likely) benign polymorphism, one recessive pathogenic variant, one likely pathogenic variant and two cell cultures containing a pathogenic variant. Fibroblasts containing either a (likely) benign polymorphism or recessive pathogenic *LMNA* c.892C>T (p.(Arg298Cys)) variant [19] ($n = 3$) and fibroblasts containing a (likely) pathogenic variant ($n = 13$) were used to calculate sensitivity and specificity of the nuclear morphology classifier. Specificity was found to be 100% (CI 29–100%) and the sensitivity was 77% (CI 46–95%). With respect to reproducibility, for two *LMNA* variants, nuclear morphology of two unrelated individuals was analyzed. Both fibroblast cell cultures with the *LMNA* c.1930C>T (p.(Arg644Cys)) variant displayed normal nuclear morphology, and nuclear morphology of two carriers of *LMNA* c.313_314delinsTT (p.(Glu105Leu)) both presented as laminopathy.

Discussion

The aim of the present study was to assess if aberrant nuclear morphology is indicative of a pathogenic *LMNA* variant and can be used to aid classification of identified genetic variants in *LMNA*. We assessed nuclear morphology of 9 laminopathy dermal fibroblast cultures and 8 control fibroblast cultures, as training set, and demonstrated that an increased percentage of abnormal nuclei, irrespective of the type of nuclear malformation (herniation, honeycomb structure or donut shape), is the most discriminating parameter between normal and laminopathy cells. Subsequent assessment of the percentage of abnormal nuclei in validation set of fibroblast cultures containing a (likely) pathogenic *LMNA* variant ($n = 13$) or a (likely) benign *LMNA* variant ($n = 3$) demonstrated a 100% specificity (CI 29–100%) with respect to determining pathogenicity, as none of the three negative samples were classified as laminopathy. However, the confidence interval is large due to limited availability of cell cultures containing (likely) benign *LMNA* variants and future inclusion of more negative samples is warranted to reduce this confidence interval. From the 13 samples containing a (likely) pathogenic *LMNA* variant, 10 samples displayed an excessive percentage of abnormal nuclei and were classified as laminopathy,

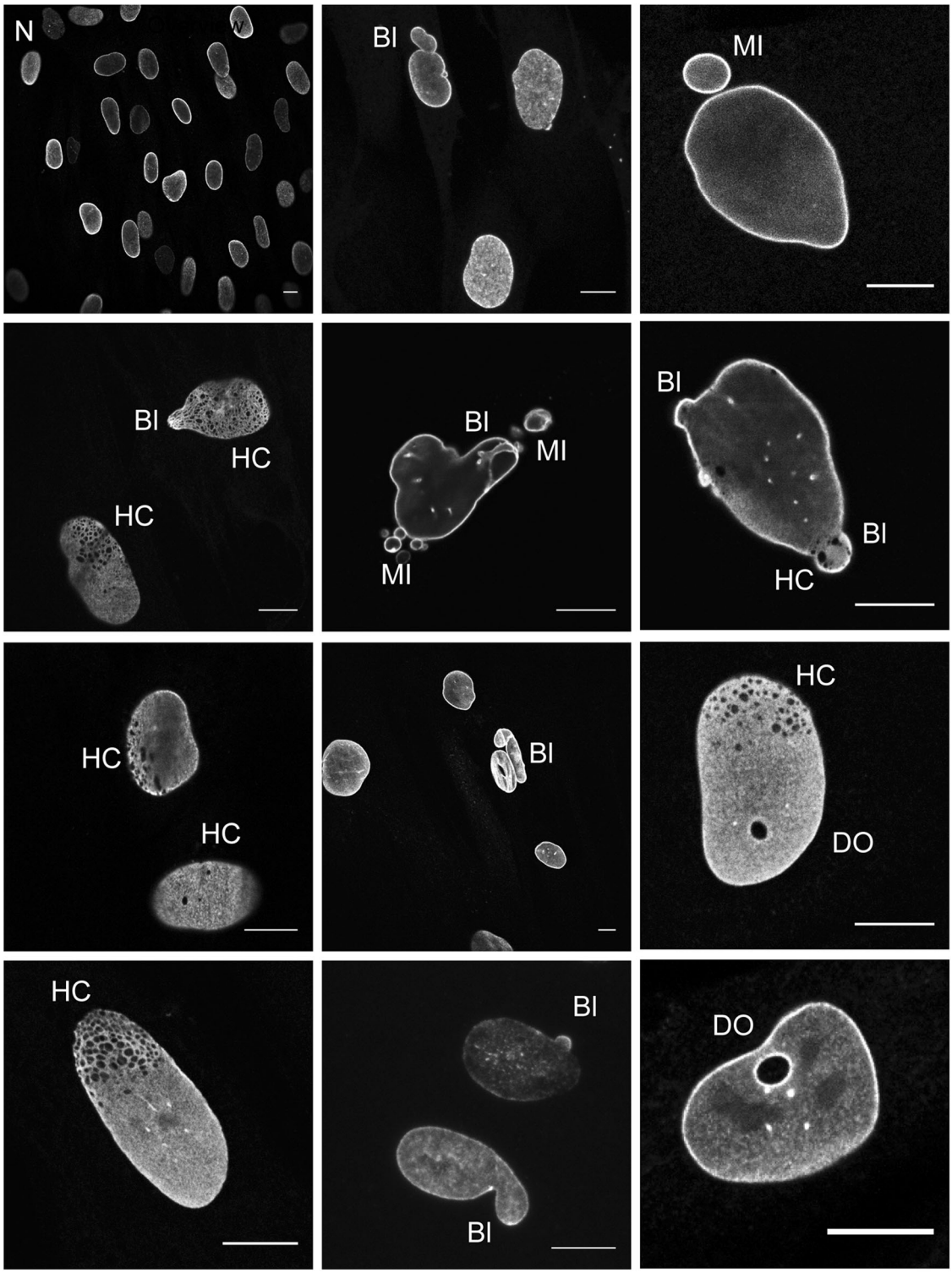

Fig. 2 Types of scored nuclear abnormalities in laminopathy cell cultures N, normal; BL, bleb; HC, honeycombs; DO, donuts, MI, micronuclei. Note that some cells contain more than 1 nuclear abnormality

resulting in a sensitivity of 77% (CI 46–95%). Moreover, the same classification was obtained for two unrelated individuals carrying the *LMNA* c.313_314delinsTT (p.(Glu105Leu)) variant for two unrelated carriers of the c.1930C>T (p.(Arg644Cys)) variant, demonstrating reproducibility of the developed method. Taken together, we

Table 2 Results nuclear morphology analysis of control- and published laminopathy fibroblasts

ID	LMNA variant[a]	Other variant[a]	% abnorm. nuclei	# total nuclei	# norm. nuclei	# abnorm. nuclei	type of abnormality[b]				
							B	HC	D	B+HC	B+D
1	p.(Lys32del)		10.67	300	268	32	19	4	8	1	0
2	p.(Tyr259*)		53.00	300	141	159	6	145	1	7	0
3	p.(Arg331Gln)		22.00	500	390	110	31	68	10	0	1
4	p.(Arg439Cys)		24.50	200	151	49	31	10	6	1	1
5	p.(Arg482Trp)		24.50	200	151	49	43	0	4	1	1
6	p.(Thr528Met)		13.50	800	692	108	29	50	18	11	0
7	p.(Thr528Met) + p.(Met540Thr)		39.80	1000	602	398	46	202	10	140	0
8	p.(Glu537Val_fs*14)		30.00	200	140	60	11	13	26	7	3
9	p.(Gly607_656del)		14.12	500	438	62	38	10	11	2	1
10	None		3.33	300	290	10	4	4	1	1	0
11	None		4.33	300	287	13	11	0	2	0	0
12	None		4.67	300	286	14	11	0	3	0	0
13	None	SCN5A p.(Phe1617del)	6.00	300	282	18	8	3	3	4	0
14	None	SCN5A p.(Phe1617del)	5.67	300	283	17	3	7	6	1	0
15	None		5.33	300	284	16	11	0	5	0	0
16	None	MYH7 p.(Ala161Pro)	5.33	300	284	16	9	1	6	0	0
17	None		3.33	300	290	10	5	1	4	0	0

[a]Protein change identified variant according to *LMNA* NG_008692.2 NM_170707.3; *SCN5A* NG_008934.1 NM_198056.2; *MYH7* NG_007884.1 NM_00257.3)

[b]Type of abnormality: B, Blebs/herniations; HC, honeycomb-like structure; D, donut-like structures, or combinations of aforementioned

conclude that a laminopathy classification based on significant number of abnormal nuclei in fibroblasts is a quick and reliable method to confirm pathogenicity and aid classification of *LMNA* variants that predict formation of aberrant lamin A/C protein, while observation of normal nuclear morphology does not rule out pathogenicity.

To our knowledge, few attempts were made to categorize laminopathies based on their nuclear abnormalities, but this is the first and largest study undertaken ($n = 45$) that uses nuclear morphology assessment of fibroblasts containing an established *LMNA* variant or no *LMNA* variant in order to rank newly identified *LMNA* variants as laminopathy or normal based on the percentage of abnormal nuclei. The percentages of abnormal nuclei observed in the control and laminopathy group in our study are in line with the percentages reported by Decaudain et al., who showed 15–25% of dysmorphic nuclei with herniations in all six patients with a *LMNA* variant compared to 5% abnormal nuclei in control fibroblasts [20]. In contrast, Muchir et al. observed <1% abnormal nuclei in controls [13], this may be a consequence of various methodological differences, criteria and sensitivity. For instance, the detection of honeycomb-like structures is highly dependent on the quality of the staining and the detection method used. Honeycomb-like structures can be missed due to a weak antibody labeling, as well as by background labeling in the affected nuclei. Moreover, most of these structures are only visible with a high-resolution oil lens, by systemically focusing individual nuclei at a number of horizontal planes. In some of our cases, confocal microscopy was needed to visualize and confirm the gaps in the lamina staining.

We observed abnormal nuclear morphology in fibroblasts containing a (likely) pathogenic variant in the *LMNA* linker or tail domain, but also for 5 out of 7 (likely) pathogenic variants located in the coil domain of *LMNA*. In contrast, Muchir et al. only observed a significantly increased percentage of abnormal nuclei in the eight cell-lines from EDMD/LGMD/FPLD patients containing a variant in the *LMNA* head or tail domain, but in none of the five *LMNA* coiled-coil domain variants [13]. Our results and those of Decaudain et al. [20] demonstrate that the presence of abnormal nuclei as a consequence of a *LMNA* pathogenic variant is not limited to certain domains of the lamin A/C protein, even if not all *LMNA* variants necessarily cause nuclear malformations, which may also be the case for the three false negative results obtained in our validation study.

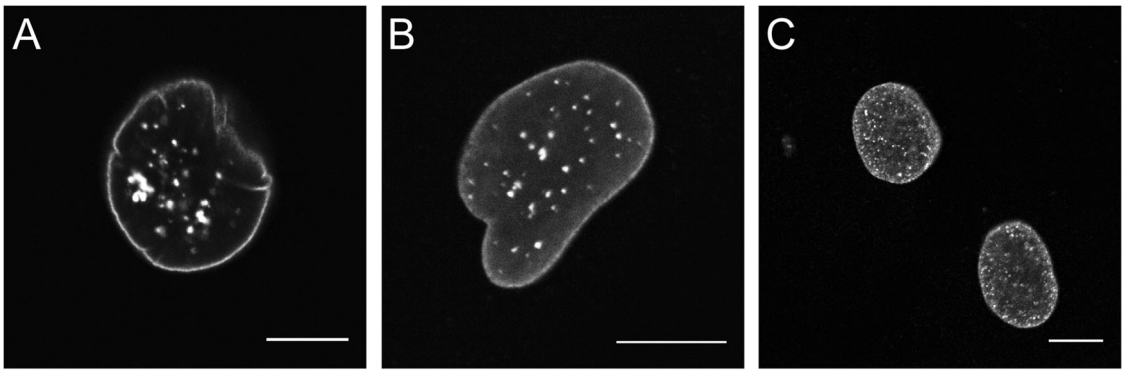

Fig. 3 Differently sized intranuclear aggregates in laminopathy cells detected with the three lamin antibodies. **a** Antibody to lamin C; **b** antibody to lamin A; **c** antibody to lamin A+C

Table 3 Quality of statistical model using different parameters

Nuclear morphology parameter	AIC[a]
Percentage of blebs	19.32
Percentage of honeycombs	16.46
Percentage of donuts	22.92
Percentage of blebs and honeycombs	22.01
Percentage of blebs and donuts	19.28
Percentage of all abnormal nuclei (blebs, donuts, and honeycombs)	4.00

[a]*AIC* Akaike information criterion; Each row of the table represents the fit of a model containing the morphological parameter mentioned in the first column. A smaller AIC denotes a better fitting model

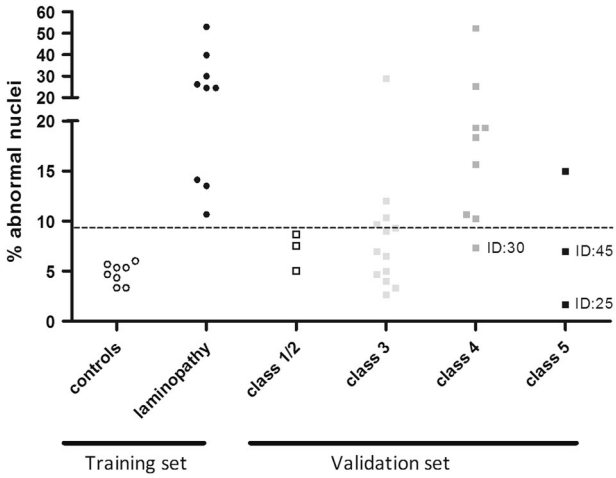

Fig. 4 Distribution of the percentage abnormal nuclei identified per class *LMNA* variant. The percentage abnormal nuclei in controls (open circles) and laminopathy patients (black circles) were used as training set to generate the classifier. The percentage of nuclear abnormalities identified in the validation set are shown grouped based on their initial clinical genetic classification: class 1/2 ((likely) benign or recessive pathogenic variants in heterozygous state) in open squares; class 3 (VUS) light gray squares; class 4 (likely pathogenic) dark gray squares; class 5 (pathogenic) black squares. The three false negative variants are indicated by their ID number

The *LMNA* c.514_1995del deletion was shown to cause haploinsufficiency [12], supporting a previous hypothesis that only formation of mutated lamin A/C proteins causes nuclear malformations, rather than a reduction in lamin A/C protein quantity, as was also observed in different tissues of mice with reduced lamin A/C expression [21]. Secondly, nuclear morphology analysis in HeLa cells transfected with p.(Arg190Trp) lamin A/C by Bhattacharjee et al. showed nuclei containing aggregates, but no other nuclear abnormalities were described and they concluded that there were no notable changes compared to wild-type [22], which is in line with our classification as normal of lamin A/C (p.(Arg190Trp)) fibroblasts. Of note, nuclear foci and/or aggregates were not taken into account in our study, but have been reported in fibroblasts [13]. Also, foci seem to arise due to overexpression, e.g., after transfection of wild-type lamin A and C [23], or much more prominently after transfection with mutant lamin constructs [8, 24]. For some *LMNA* variants it has been reported that mutated lamin can form aggregates without interacting with wild-type lamins and thus possibly causing no harm to the nuclear shape nor integrity [25]. In our study, aggregates were only detected in c.1634G>A (p.(Arg545His)) fibroblasts, which also presented with some honeycomb and donut-like structures and a classifier score of 0.51, which we considered as "unclassified". Future inclusion of nuclear aggregates as parameter may increase sensitivity of the classification tool, but requires further research to establish the occurrence of foci in wild-type cells and a systemic assessment of their significance. Exploring implementation of automated quantification of nuclear morphology in 2D microscopy images, as performed by Core et al. to identify dysmorphic nuclei [26], may also aid our nuclear morphology analysis procedure and classification tool further, but requires optimization as honeycomb structures are difficult to assess using 2D images and likely require 3D analysis methods. Also, automated analysis may pose challenges for implementation of the nuclear morphology analysis in routine

Table 4 Results nuclear morphology analysis in validation study

ID	LMNA variant[a]	Predicted effect on protein level	LMNA domain[b]	References	Initial classification[c]	% abnormal nuclei	Total # nuclei	# normal nuclei	# abnormal nuclei	Nuclear morphology classifier (score)	Age at biosy	Fibroblast passage nr.	Sex	Phenotype
18	No LMNA variant			NA	--	7.50	200	185	15	Normal (0.00)	38	3	Female	Partial lipodystrophy
44	c.1968 + 26A>G			NA	1	8.67	300	274	26	Normal (0.00)	52	2	Male	DCM
29	c.892C > T+EMD c.110-112del	p.(Arg298Cys) + EMD p.(Lys37del)	Coil 2	[30]	2 (5AR)[d] 2 (5 X-linked)	5.00	200	184	16	Normal (0.00)	41	7	Female	ACD
35	c.1619T > C	p.(Met540Thr)	Tail	[3, 31, 38]	3 (5 AR)[e]	9.00	600	546	54	Normal (0.01)	32	5	Female	none
27	c.737A > G	p.(Gln246Arg)	Coil 2	NA	3	4.00	200	192	8	Normal (0.00)	48	3	Male	LVNC
36	c.161C > T	p.(Thr54Met)	Coil 1a	NA	3	7.00	300	279	21	Normal (0.00)	62	3	Male	HCM
38	c.1718C > T	p.(Ser573Leu)	Tail	[43, 44]	3	4.67	300	286	14	Normal (0.00)	45	4	Male	LQT
40	c.1786_1800del	p.(Asp596_Ala600del)	Tail	NA	3	5.00	300	285	15	Normal (0.00)	17	3	Male	NCCM
41	c.1879C > T	p.(Arg627Cys)	Tail	[45]	3	6.50	600	561	39	Normal (0.00)	54	4	Male	none
42	c.1930C > T	p.(Arg644Cys)	Tail	[46–48]	3	2.67	300	292	8	Normal (0.00)	59	5	Male	LGMD, CM
43	c.1930C > T	p.(Arg644Cys)	Tail	[46–48]	3	3.33	300	290	10	Normal (0.00)	33	2	Male	VF, HCM
30	c.949G > A	p.(Glu317Lys)	Coil 2	[27, 28, 49]	4	7.33	300	278	22	Normal (0.00)	60	3	Female	DCM
25	c.568C > T	p.(Arg190Trp)	Coil 1b	[22, 27, 50]	5	1.67	300	295	5	Normal (0.00)	34	3	Male	DCM
45	c.514_1995del	Haploinsuffiency		[12]	5	7.00	300	279	21	Normal (0.00)	50	3	Male	AF
37	c.1634G > A	p.(Arg545His)	Tail	[51–53]	3	9.33	300	272	28	Unclassified (0.51)	42	3	Female	LVNC
19	c.208G > A	p.(Val70Ile)	Coil 1a	NA	3	29.00	300	213	87	Laminopathy (1.00)	42	3	Male	DCM
20	c.236C > A	p.(Ala79Asp)	Coil 1b	NA	3	10.33	300	269	31	Laminopathy (1.00)	59	3	Male	DCM
32	c.1201C > T	p.(Arg401Cys)	Tail	[40, 49, 54, 55]	3	9.67	300	271	29	Laminopathy (0.99)	78	4	Male	DCM
39	c.173G > T	p.(Gly58Val)	Coil 1a	NA	3	12.00	300	264	36	Laminopathy (1.00)	52	4	Female	ARVC
21	c.247delinsCC	p.(Ala83Profs*11)	Coil1b	NA	4	25.33	300	224	76	Laminopathy (1.00)	46	5	Female	DCM
22	c.313_314delinsTT	p.(Glu105Leu)	Coil 1b	NA	4	10.25	400	359	41	Laminopathy (1.00)	70	3	Male	DCM
23	c.313_314delinsTT	p.(Glu105Leu)	Coil 1b	NA	4	18.33	300	245	55	Laminopathy (1.00)	46	3	Male	DCM, AF, mitralis insuf.
26	c.647G > A	p.(Arg216His)	Coil 1b	NA	4	15.67	300	253	47	Laminopathy (1.00)	63	3	Male	DCM

Table 4 (continued)

ID	LMNA variant[a]	Predicted effect on protein level	LMNA domain[b]	References	Initial classification[c]	% abnormal nuclei	Total # nuclei	# normal nuclei	# abnormal nuclei	Nuclear morphology classifier (score)	Age at biosy	Fibroblast passage nr.	Sex	Phenotype
28	c.810G > A	r.766_810del45		[56]	4	52.33	300	143	157	Laminopathy (1.00)	30	2	Female	DCM, muscle weakness
33	c.1300G > A	p.(Ala434Thr)	Tail	NA	4	19.33	300	242	58	Laminopathy (1.00)	50	4	Male	DCM, VF
34	c.1592_1594del	p.(Ile531del)	Tail	NA	4	10.67	300	268	32	Laminopathy (1.00)	44	2	Female	EDMD
31[f]	c.[992G > A]; [1879C > T]	p.[(Arg331Gln)]; [(Arg627Cys)]	Coil 2 + Tail	[33–35]	4 3	19.33	500	350	150	Laminopathy (1.00)	53	3	Male	DCM
24	c.481G > A	p.(Glu161Lys)	Coil 1b	[22, 50, 57]	5	15.00	300	255	45	Laminopathy (1.00)	53	3	Male	DCM, VF

ACD atrial cardiac disease, *AF* atrial fibrillation, *AR* autosomal recessive inheritance, *ARVC* Arrhythmogenic right ventricle cardiomyopathy, *CM* cardiomyopathy, *DCM* dilated cardiomyopathy, *EDMD* emery dreifuss muscular dystrophy, *HCM* hypertrophic cardiomyopathy, *LVNC* left ventricle non-compaction, *VF* ventricular fibrillation, *X-linked* X-linked inheritance

[a]DNA and predicted protein change of identified variant according to *LMNA* NG_008692.2 NM_170707.3, EMD NG_008677.1 NM_000117.2. All variants were identified heterzygously

[b]Affected protein domain according to Nextprot structures LMNA isoform A

[c]Initial classification of genetic variant reported to clinican prior to nuclear morphology analysis, class 1: benign variant, class 2: likely benign variant, class 3: variant of unknown significance, class 4: likely pathogenic variant, class 5: pathogenic variant

[d]Heterozygous variant and no second LMNA variant demonstrated. This variant has only been demonstrated to cause disease in homozygous state, but no functional effect has been demonstrated in heterozygous state and is regarded as likely benign in the analysis

[e]Heterozygous variant and no second LMNA variant demonstrated. This variant has been shown to cause disease in compound heterozygous form (ID7), but the functional effect in heterozygous form is unclear and is included als class 3 (VUS) in current analysis

[f]ID31 compound heterozyous carrier of two LMNA variants, these variants were tested in isolation in ID 3 and ID 41

genetic laboratories, as the required equipment may not be available. Thirdly, some *LMNA* pathogenic variants may not cause nuclear abnormalities at all or only cause nuclear abnormalities following stress or present in certain cell-types other than fibroblasts. This may be the case for the likely pathogenic variant c.949G>A (p.(Glu317Lys)), which has been reported in patients with AV-block and DCM [27, 28]. It is unclear if this variant can cause nuclear abnormalities at all, since it has not been functionally analyzed by other groups. Further research is required to assess pathogenicity of this variant and its mode of action.

Taken together, normal nuclear morphology does not rule out pathogenicity of *LMNA* variants, but detection of excessive abnormal nuclei provides functional evidence of pathogenicity and may warrant reclassification of *LMNA* VUS as a pathogenic variant. Implementation of this tool in our laboratory enabled reclassification of 4 of the 12 variants from VUS to likely pathogenic variant (33%). Since ~50% of all identified rare missense and splice-site variants in *LMNA* are being classified as VUS, implementation of this nuclear morphology analysis tool, will have considerable impact on the counseling and follow-up for patients and family members.

Acknowledgements We would like to thank all persons (A. Bardai, G. Bonne, B. van Engelen, D De Jongh, P. Helderman, R. Hennekam, D. Koolen, C. Marcelis, S. Sallevelt, K. van Kaam, E. Vanhoutte) that provided the fibroblasts included in this study.

Compliance with ethical standards

Conflict of interest The authors declare that they have no conflict of interest.

References

1. Worman HJ. Nuclear lamins and laminopathies. J Pathol. 2012;226:316–25.
2. Gonzalo S, Kreienkamp R, Askjaer P. Hutchinson-Gilford Progeria syndrome: a premature aging disease caused by LMNA gene mutations. Ageing Res Rev. 2017;33:18–29.
3. Verstraeten VL, Broers JL, van Steensel MA, et al. Compound heterozygosity for mutations in LMNA causes a progeria syndrome without prelamin A accumulation. Hum Mol Genet. 2006;15:2509–22.
4. Carboni N, Politano L, Floris M, et al. Overlapping syndromes in laminopathies: a meta-analysis of the reported literature. Acta Myol. 2013;32:7–17.
5. Brodsky GL, Muntoni F, Miocic S, et al. Lamin A/C gene mutation associated with dilated cardiomyopathy with variable skeletal muscle involvement. Circulation. 2000;101:473–6.
6. Richards S, Aziz N, Bale S, et al. Standards and guidelines for the interpretation of sequence variants: a joint consensus recommendation of the American College of Medical Genetics and Genomics and the Association for Molecular Pathology. Genet Med. 2015;17:405–24.
7. Caux F, Dubosclard E, Lascols O, et al. A new clinical condition linked to a novel mutation in lamins A and C with generalized lipoatrophy, insulin-resistant diabetes, disseminated leukomelanodermic papules, liver steatosis, and cardiomyopathy. J Clin Endocrinol Metab. 2003;88:1006–13.
8. Favreau C, Dubosclard E, Ostlund C, et al. Expression of lamin A mutated in the carboxyl-terminal tail generates an aberrant nuclear phenotype similar to that observed in cells from patients with Dunnigan-type partial lipodystrophy and Emery-Dreifuss muscular dystrophy. Exp Cell Res. 2003;282:14–23.
9. Novelli G, Muchir A, Sangiuolo F, et al. Mandibuloacral dysplasia is caused by a mutation in LMNA-encoding lamin A/C. Am J Hum Genet. 2002;71:426–31.
10. Vigouroux C, Auclair M, Dubosclard E, et al. Nuclear envelope disorganization in fibroblasts from lipodystrophic patients with heterozygous R482Q/W mutations in the lamin A/C gene. J Cell Sci. 2001;114:4459–68.
11. Fidzianska A, Bilinska ZT, Tesson F, et al. Obliteration of cardiomyocyte nuclear architecture in a patient with LMNA gene mutation. J Neurol Sci. 2008;271:91–6.
12. Gupta P, Bilinska ZT, Sylvius N, et al. Genetic and ultrastructural studies in dilated cardiomyopathy patients: a large deletion in the lamin A/C gene is associated with cardiomyocyte nuclear envelope disruption. Basic Res Cardiol. 2010;105:365–77.
13. Muchir A, Medioni J, Laluc M, et al. Nuclear envelope alterations in fibroblasts from patients with muscular dystrophy, cardiomyopathy, and partial lipodystrophy carrying lamin A/C gene mutations. Muscle Nerve. 2004;30:444–50.
14. Houben F, Ramaekers FC, Snoeckx LH, et al. Role of nuclear lamina-cytoskeleton interactions in the maintenance of cellular strength. Biochim Biophys Acta. 2007;1773:675–86.
15. Claes GR, van Tienen FH, Lindsey P, et al. Hypertrophic remodelling in cardiac regulatory myosin light chain (MYL2) founder mutation carriers. Eur Heart J. 2016;37:1815–22.
16. Dyer JA, Kill IR, Pugh G, et al. Cell cycle changes in A-type lamin associations detected in human dermal fibroblasts using monoclonal antibodies. Chromosome Res. 1997;5:383–94.
17. Akaike H. Information theory and an extension of the maximum likelihood principle. In: Petrov BN, Csàki F, editors. Second International Symposium on Inference Theory: Akadémiai Kiadó, Budapest; 1973; p 267–81.
18. Ihaka R, Gentleman R. R: a language for data analysis and graphics. J Comput Graph Stat. 1996;5:299–314.
19. Ben Yaou R, Toutain A, Arimura T, et al. Multitissular involvement in a family with LMNA and EMD mutations: Role of digenic mechanism? Neurology. 2007;68:1883–94.
20. Decaudain A, Vantyghem MC, Guerci B, et al. New metabolic phenotypes in laminopathies: LMNA mutations in patients with severe metabolic syndrome. J Clin Endocrinol Metab. 2007;92:4835–44.
21. Sullivan T, Escalante-Alcalde D, Bhatt H, et al. Loss of A-type lamin expression compromises nuclear envelope integrity leading to muscular dystrophy. J Cell Biol. 1999;147:913–20.
22. Bhattacharjee P, Banerjee A, Banerjee A, et al. Structural alterations of Lamin A protein in dilated cardiomyopathy. Biochemistry. 2013;52:4229–41.
23. Broers JL, Machiels BM, van Eys GJ, et al. Dynamics of the nuclear lamina as monitored by GFP-tagged A-type lamins. J Cell Sci. 1999;112(Pt 20):3463–75.
24. Broers JL, Kuijpers HJ, Ostlund C, et al. Both lamin A and lamin C mutations cause lamina instability as well as loss of internal nuclear lamin organization. Exp Cell Res. 2005;304:582–92.
25. Roblek M, Schuchner S, Huber V, et al. Monoclonal antibodies specific for disease-associated point-mutants: lamin A/C R453W and R482W. PLoS One. 2010;5:e10604.

26. Core JQ, Mehrabi M, Robinson ZR, et al. Age of heart disease presentation and dysmorphic nuclei in patients with LMNA mutations. PLoS One. 2017;12:e0188256.
27. Arbustini E, Pilotto A, Repetto A, et al. Autosomal dominant dilated cardiomyopathy with atrioventricular block: a lamin A/C defect-related disease. J Am Coll Cardiol. 2002;39:981–90.
28. Villa F, Maciag A, Spinelli CC, et al. A G613A missense in the Hutchinson's progeria lamin A/C gene causes a lone, autosomal dominant atrioventricular block. Immun Ageing. 2014;11:19.
29. Vytopil M, Benedetti S, Ricci E, et al. Mutation analysis of the lamin A/C gene (LMNA) among patients with different cardiomuscular phenotypes. J Med Genet. 2003;40:e132.
30. Muchir A, van Engelen BG, Lammens M, et al. Nuclear envelope alterations in fibroblasts from LGMD1B patients carrying nonsense Y259X heterozygous or homozygous mutation in lamin A/C gene. Exp Cell Res. 2003;291:352–62.
31. De Vos WH, Houben F, Kamps M, et al. Repetitive disruptions of the nuclear envelope invoke temporary loss of cellular compartmentalization in laminopathies. Hum Mol Genet. 2011;20: 4175–86.
32. van Spaendonck-Zwarts KY, van Rijsingen IA, van den Berg MP, et al. Genetic analysis in 418 index patients with idiopathic dilated cardiomyopathy: overview of 10 years' experience. Eur J Heart Fail. 2013;15:628–36.
33. Moller DV, Pham TT, Gustafsson F, et al. The role of Lamin A/C mutations in Danish patients with idiopathic dilated cardiomyopathy. Eur J Heart Fail. 2009;11:1031–5.
34. Gangemi F, Degano M. Disease-associated mutations in the coil 2B domain of human lamin A/C affect structural properties that mediate dimerization and intermediate filament formation. J Struct Biol. 2013;181:17–28.
35. Hoorntje ET, Bollen IA, Barge-Schaapveld DQ, et al. Lamin A/C-related cardiac disease: late onset with a variable and mild phenotype in a large cohort of patients with the lamin A/C p.(Arg331Gln) founder mutation. Circ Cardiovasc Genet. 2017;10: DOI: 10.1161/CIRCGENETICS.116.001631 1–10.
36. Verstraeten VL, Caputo S, van Steensel MA, et al. The R439C mutation in LMNA causes lamin oligomerization and susceptibility to oxidative stress. J Cell Mol Med. 2009;13:959–71.
37. Shackleton S, Lloyd DJ, Jackson SN, et al. LMNA, encoding lamin A/C, is mutated in partial lipodystrophy. Nat Genet. 2000;24:153–6.
38. Saj M, Dabrowski R, Labib S, et al. Variants of the lamin A/C (LMNA) gene in non-valvular atrial fibrillation patients: a possible pathogenic role of the Thr528Met mutation. Mol Diagn Ther. 2012;16:99–107.
39. Renou L, Stora S, Yaou RB, et al. Heart-hand syndrome of Slovenian type: a new kind of laminopathy. J Med Genet. 2008;45:666–71.
40. Houben F, De Vos WH, Krapels IP, et al. Cytoplasmic localization of PML particles in laminopathies. Histochem Cell Biol. 2013;139:119–34.
41. De Sandre-Giovannoli A, Bernard R, Cau P, et al. Lamin a truncation in Hutchinson-Gilford progeria. Science. 2003;300: 2055.
42. Bruston F, Delbarre E, Ostlund C, et al. Loss of a DNA binding site within the tail of prelamin A contributes to altered heterochromatin anchorage by progerin. FEBS Lett. 2010;584:2999–3004.
43. Taylor MR, Fain PR, Sinagra G, et al. Natural history of dilated cardiomyopathy due to lamin A/C gene mutations. J Am Coll Cardiol. 2003;41:771–80.
44. Benedetti S, Menditto I, Degano M, et al. Phenotypic clustering of lamin A/C mutations in neuromuscular patients. Neurology. 2007;69:1285–92.
45. Kumar S, Baldinger SH, Gandjbakhch E, et al. Long-term arrhythmic and nonarrhythmic outcomes of lamin A/C mutation carriers. J Am Coll Cardiol. 2016;68:2299–307.
46. Genschel J, Bochow B, Kuepferling S, et al. A R644C mutation within lamin A extends the mutations causing dilated cardiomyopathy. Hum Mutat. 2001;17:154.
47. Cann F, Corbett M, O'Sullivan D, et al. Phenotype-driven molecular autopsy for sudden cardiac death. Clin Genet. 2017;91:22–9.
48. Nouhravesh N, Ahlberg G, Ghouse J, et al. Analyses of more than 60,000 exomes questions the role of numerous genes previously associated with dilated cardiomyopathy. Mol Genet Genom Med. 2016;4:617–23.
49. Walsh R, Thomson KL, Ware JS, et al. Reassessment of Mendelian gene pathogenicity using 7855 cardiomyopathy cases and 60,706 reference samples. Genet Med. 2017;19:192–203.
50. Banerjee A, Rathee V, Krishnaswamy R, et al. Viscoelastic behavior of human lamin A proteins in the context of dilated cardiomyopathy. PLoS One. 2013;8:e83410.
51. van Rijsingen IA, Nannenberg EA, Arbustini E, et al. Gender-specific differences in major cardiac events and mortality in lamin A/C mutation carriers. Eur J Heart Fail. 2013;15:376–84.
52. Olfson E, Cottrell CE, Davidson NO, et al. Identification of medically actionable secondary findings in the 1000 genomes. PLoS One. 2015;10:e0135193.
53. Chan D, McIntyre AD, Hegele RA, et al. Familial partial lipodystrophy presenting as metabolic syndrome. J Clin Lipidol. 2016;10:1488–91.
54. Hanisch F, Neudecker S, Wehnert M, et al. [Hauptmann-Thannhauser muscular dystrophy and differential diagnosis of myopathies associated with contractures]. Nervenarzt. 2002;73: 1004–11.
55. Yang L, Munck M, Swaminathan K, et al. Mutations in LMNA modulate the lamin A—Nesprin-2 interaction and cause LINC complex alterations. PLoS One. 2013;8:e71850.
56. Scharner J, Brown CA, Bower M, et al. Novel LMNA mutations in patients with Emery-Dreifuss muscular dystrophy and functional characterization of four LMNA mutations. Hum Mutat. 2011;32:152–67.
57. Sebillon P, Bouchier C, Bidot LD, et al. Expanding the phenotype of LMNA mutations in dilated cardiomyopathy and functional consequences of these mutations. J Med Genet. 2003;40:560–7.
58. Stenson PD, Ball EV, Mort M, et al. The Human Gene Mutation Database (HGMD) and its exploitation in the fields of personalized genomics and molecular evolution. Curr Protoc Bioinform. 2012;Chapter 1: Unit113.